Progress In Electromagnetics Research Letters, Vol. 77, 109–115, 2018

Terahertz Polariton Dispersion in Uniaxial Optical Crystals

Seiji Kojima*

Abstract—Phonon-polariton is the coupled excitation between optical phonon and photon. The remarkable frequency vs. wavevector dispersion relation of phonon-polariton contributes to important technological applications such as tunable terahertz radiation sources and basic materials science to clarify the terahertz dynamics of condensed matter such as lattice instability in ferroelectrics. This paper studies the broadband dispersion relation of phonon-polariton between $10\,\mathrm{cm}^{-1}$ and $1200\,\mathrm{cm}^{-1}$ in uniaxial ferroeletric crystals, $LiNbO_3$ (LN) and $LiTaO_3$ (LT) with polar trigonal system on the basis of the observed results using THz-Raman spectroscopy, THz time domain spectroscopy, and far-infrared spectroscopy. The dispersion on the lowest-frequency TO mode with $A_1(z)$ symmetry of LN and LT crystals, which are assigned as ferroelectric soft modes, is discussed.

1. INTRODUCTION

In condensed matter, infrared active optical phonons strongly couple to photons with nearly the same wavevector and energy. This mixed elementary excitation is known as a phonon-polariton [1, 2]. Lithium niobate (LN), $LiNbO_3$, and lithium tantalite (LT), $LiTaO_3$ of ilmenite like structure, are typical technologically important uniaxial ferroelectric materials for not only piezoelectric devices such as SAW filter, ultrasonic transducer but also optical devices such as laser beam deflectors, optical shutters, and broadband terahertz generators [3, 4]. For the study of optical application, the optional properties in the large frequency range are very important, while the broadband studies of phonon-polariton in the terahertz range are still not enough.

In the present paper, the various experimental methods to observe the dispersion relation of phonon-polariton are reviewed. Then the experimental results of optical uniaxial crystals, ferroelectric lithium niobate $LiNbO_3$ (LN) and ferroelectric lithium tantalate $LiTaO_3$ (LT) with trigonal system using the FTIR spectroscopy of the far- and mid-IR regions, terahertz time-domain spectroscopy (THz-TDS), and forward THz-Raman scattering are discussed.

2. EXPERIMENTAL METHODS TO OBSERVE PHONON-POLARITON

When infrared active optical phonons are incident to condensed matter, they strongly couple to photons with nearly the same wavevector and energy, and propagate as the mixed excitation called phonon-polariton [1]. The phonon-polariton dispersion relation is notable only in the polariton wavevectors, which are much smaller than that of visible light. Therefore, the polariton dispersion cannot be detected in the standard Raman scattering experiments using back or right angle scattering geometry in which the magnitude of wavevectors of scattered excitation is much larger. Up to the present, in most of the experimental studies on polaritons the dispersion relation of phonon-polariton has been studied using forward Raman scattering [5] and impulsive stimulated Raman scattering (ISRS) [6]. According to the selection rule, Raman scattering spectroscopy can detect only phono-polariton which is both

Received 5 May 2018, Accepted 18 July 2018, Scheduled 30 July 2018
* Corresponding author: Seiji Kojima (kojima@ims.tsukuba.ac.jp).
The author is with the Division of Materials Science, University of Tsukuba, Tsukuba, Ibaraki 305-8573, Japan.

infrared active and Raman active. However, in a centrosymmetric crystal, the exclusion rule gives no Raman active mode for all the infrared active modes. Therefore, the Raman study on phonon-polaritons has been appliedto non-centrosymmetric polar crystals. However, in most of the applications of phonon-polariton, the ferroelectric crystals with polar symmetry have been studied, and Raman scattering spectroscopy is a powerful tool for the experimental study on the dispersion relation of phonon-polariton [2].

For the observation of polariton related to a diagonal Raman tensor component, the polarization planes of incident and scattered light are parallel, and the observation of small polariton wavevectors is possible. In the early stage of phonon-polariton studies, infrared (IR) and far-IR spectroscopy was also used [7]; however, the detailed comparison among other spectroscopic methods was not enough.

In Raman scattering, by the conservation law of wavevectors as shown in Fig. 1, the magnitude of polariton wavevector k_p is given by the magnitude of wavevectors of incident light k_i, scattered light k_s, and the scattering angle θ between them.

$$k_p^2 = k_i^2 + k_s^2 - 2k_i k_s \cos\theta. \tag{1}$$

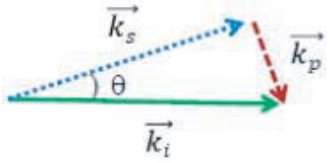

Figure 1. The conservation law of wavevectors among incident light k_i, scattered light k_s, and polarion k_p.

Polariton dispersion relation has been studied to measure Raman scattering spectra as a function of the scattering angle θ [2, 8].

For example, the $A_1(z)$ symmetry phonon-polariton is observed through the diagonal Raman tensor component R_{cc} for the point group C_{3v}. The Raman scattering spectra of the $A_1(z)$ symmetry phonon-polariton can be measured at the forward scattering geometry, $a(cc)a+\Delta b$. The magnitude of polariton wavevector q with $A_1(z)$ symmetry is given by

$$\begin{aligned} k_p^2 &= (2\pi n_e/\lambda_i)^2 + (2\pi n_e/\lambda_s)^2 - 2(2\pi n_e)^2/\lambda_i\lambda_s\cos\theta \\ &\approx 8\pi^2 n_e^2(1-\cos\theta)/\lambda_i^2 \approx 4\pi^2 n_e^2\theta^2/\lambda_i^2, \quad \text{for} \quad k_p \ll 1, \end{aligned} \tag{2}$$

where λ_i and λ_s are wavelengths of incident and scattered lights, respectively, and n_e is the refractive index of extraordinary ray. According to Equation (2), the observation of polariton down to $q = 0$ is possible, if the intense elastic scattering is well removed in the measurement.

According to Born and Huang's analysis [1], the dispersion relation of polariton was given by the equation, $\varepsilon(k,\omega) = c^2k^2/\omega^2$ where ω, k, c, and $\varepsilon(k,\omega)$ are angular frequency, wave vector, light velocity, and dielectric constant, respectively. Fig. 2 shows the polariton dispersion relation when two infrared active optical modes exist, where $\omega_{\mathrm{TO1}} = 200\,\mathrm{cm}^{-1}$, $\omega_{\mathrm{LO1}} = 230\,\mathrm{cm}^{-1}$, $\omega_{\mathrm{TO2}} = 660\,\mathrm{cm}^{-1}$, and $\omega_{\mathrm{LO2}} = 830\,\mathrm{cm}^{-1}$. The dotted lines show the observable region by forward Raman scattering experiments. In LN and LT crystals with the point group C_{3v} at room temperature, the polariton peak of $A_1(z)$ symmetry can be observed in forward Raman scattering experiments [2, 8]. In infrared spectroscopy, the polariton absorption of $A_1(z)$ symmetry can be observed under the condition of polarization $E//z$.

In far-infrared and infrared spectroscopy for the observation of the polariton dispersion relation, the reflection measurements of the strong absorption caused the difficulty to determine the polariton-dispersion accurately. On the other hand, the recent progress of Terahertz-time domain spectroscopy (THz-TDS) using a coherent far-infrared light source is a new tool to observe infrared active modes in a far-infrared region [9]. The recent improvement in the coherent terahertz generation using a femtosecond pulse laser enables a unique determination of a complex dielectric constant without the use of Kramers-Kronig transformation, and THz-TDS has attracted much attention, while the frequency range is limited below 2–3 tarehertz.

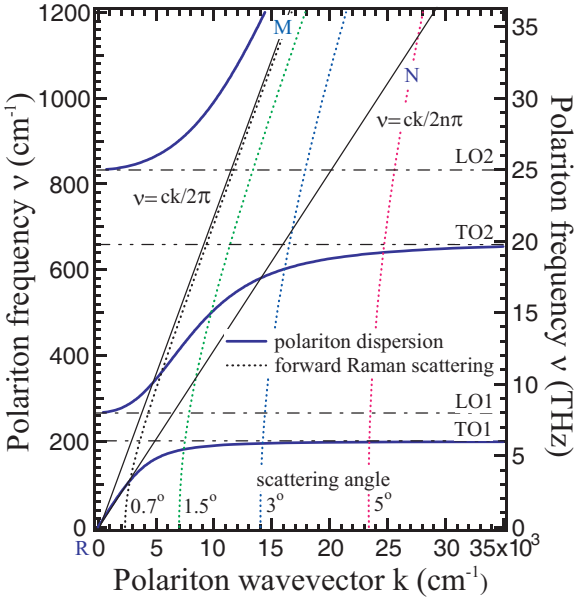

Figure 2. Calculated dispersion relations of phonon polariton frequency against polariton wavevector. The slopes of lines RM and RN are $\frac{1}{\sqrt{\varepsilon_\infty}}$ and $\frac{1}{\sqrt{\varepsilon_0}}$, respectively, where ε_∞ and ε_0 are the dielectric constants at infinity and very low-frequency, respectively.

Recently, a far-infrared spectroscopic ellipsometry (FIRSP) system has been developed by the combination of a far-infrared spectrometer and an ellipsometry [10]. The Michelson interferometer of the Fourier transform spectrometer is followed by a rotating analyzer type ellipsometer. The light source is a high-pressure mercury lamp, and the detector is a Si bolometer unit, which enables us to measure a far-infrared spectrum in the low-frequency region. The reflected light was elliptically polarized owing to the difference in complex reflection coefficient between the p- and s-polarizations. The lights of the p- and s-polarized components were individually measured by a rotating wiregrid analyzer in the frequency range, and the accurate determination of real and imaginary parts of dielectric constants can be possible in the frequency range from 40 to 700 cm^{-1} without the use of Kramers-Kronig transformation. In most cases, the frequency range of optical modes in ABO_3 type ferroelectrics is 30 to 800 cm^{-1}; therefore, it is certain that FIRSP is a powerful experimental method to study the broadband dispersion relation of phonon-polariton.

3. EXPERIMENTAL OBSERVATION OF PHONON-POLARITON

LN and LT are called multi-talented crystals, because of their many applications by the outstanding piezoelectric, pyroelectric, electro-optic, and nonlinear-optic effects. However, there are still some problems in the characterization of their high-frequency dielectric properties. LN and LT undergo ferroelectric transitions, and spontaneous polarization appears in a ferroelectric phase at room temperature. In ferroelectric LN and LT crystals with C_{3v} symmetry at room temperature, the symmetry of 27 optical modes is given by

$$4A_1(z) + 9E(x, y) + 5A_2, \tag{3}$$

where four $A_1(z)$ and nine $E(x, y)$ modes are infrared active and propagate as polariton in medium [11–13]. The ferroelectric axis is z-axis. Five A_2 modes are silent modes. Among these modes, $E(x, y)$ and $A_1(z)$ symmetry modes are both Raman and IR active. In the present study, the broadband polariton dispersion relation is discussed for $A_1(z)$ modes of LN and LT using the experimental results by various spectroscopic methods in the frequency range between 10 cm^{-1} and 1200 cm^{-1}.

3.1. Phonon Polariton Dispersion of Lithium Niobate with A_1(z) Symmetry

In ferroelectric LN crystals, there are four normal modes with $A_1(z)$ symmetry at room temperature. These four modes were clearly observed in both backward Raman scattering and reflection IR spectra [10]. The mode frequencies of four modes are in agreement with the values reported in literature [14]. By the combination with the observed polariton dispersion relations determined by forward Raman scattering [15], terahertz time-domain spectroscopy [12, 17] and far-infrared spectroscopic ellipsometry [10], the broadband polariton dispersion relation with $A_1(z)$ symmetry between $10\,\mathrm{cm}^{-1}$ and $1200\,\mathrm{cm}^{-1}$ is shown in Fig. 3. In the analysis of Raman scattering spectra, the polariton wavevector is a real number, while the polariton frequency is a complex number. The imaginary part of frequency is the damping factor, which is related to the temporal decay of polariton propagation. The damping factor is proportional to the width of a polariton peak in a Raman spectrum, if there is no uncertainty of polariton wavevector, and spectral resolution is negligible. However, actually the uncertainty of polariton wave vector is not negligible owing to the uncertainty of the scattering angle. Therefore, we discuss only about polariton dispersion of real polariton wavevector. Since the scattering intensity of polariton is very weak, it is difficult to reduce the uncertainty of the scattering angle θ.

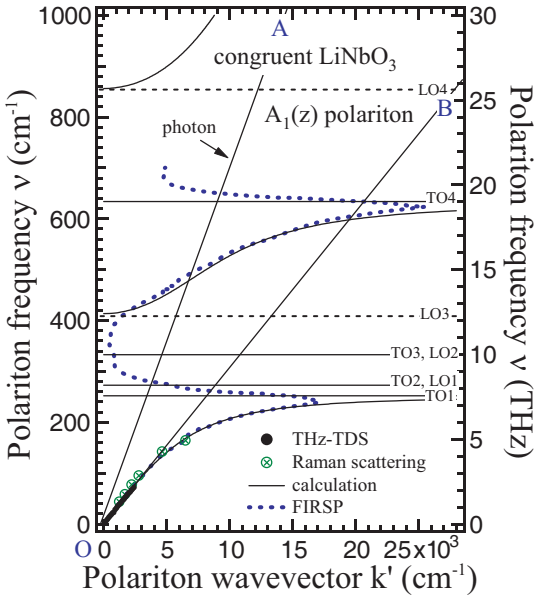

Figure 3. Observed dispersion relations of phonon polariton frequency with $A_1(z)$ symmetry of $LiNbO_3$ against real part of polariton wavevector. The slopes of lines OA and OB are $\frac{1}{\sqrt{\varepsilon_\infty}}$ and $\frac{1}{\sqrt{\varepsilon_0}}$, respectively.

Figure 3 shows the real part of polariton wave vector against the polariton frequency with $A_1(z)$ symmetry. The solid lines denote the calculated dispersion with no polariton damping using the following equation,

$$\varepsilon\left(k,\omega\right)=\frac{c^2k^2}{\omega^2}=\varepsilon(\infty)\prod_i\left(\omega_{LOi}^2-\omega^2\right)/\prod_i\left(\omega_{TOi}^2-\omega^2\right), \tag{4}$$

where ω_{Toi} and ω_{LOi} denote the mode frequency of i-th TO and i-th LO modes.

The values of TO and LO mode frequencies of LN are listed in Table 1. Closed green circles denote the values observed by the forward Raman scattering measurements [15, 16]. Using the observed values of complex dielectric constant of LN by FIRSP [10], the complex refractive index $n(k,\omega)+i\kappa(k,\omega)$ was determined by the following equation,

$$\varepsilon(k,\omega)=\{n(k,\omega)+i\kappa(k,\omega)\}^2. \tag{5}$$

The polariton dispersion relation for real part of polariton wavevector k' was determined by the equation $k'=\omega n(k,\omega)/c$. Blue dotted curve shows the results determined by FIRSP. The complex

Table 1. Mode frequencies of TO and LO modes with $A_1(z)$ symmetry of a congruent lithium niobate crystal, where the unit is THz.

	1	2	3	4
ω_{TO}	7.54	8.17	9.97	19.0
ω_{LO}	8.16	9.96	12.4	25.7

dielectric constant was determined by THz-TDS using the transmitted amplitude and the phase delay of THz waves, and the plariton dispersion relation was also determined below 2 THz [12]. Black closed circles show the observed values by THz-TDS. These plots determined using the observed results by forward Raman scattering, FIRSP, and THz-TDS are in good agreement with the calculated values.

By the heterodyned impulsive stimulated Raman scattering (ISRS) measurement of the LN crystal, Bakker et al. observed resonances, whose origin was attributed to the cross-anharmonic couplings between different normal-mode lattice vibrations [18]. However, such anomaly was not observed in the subsequent impulsive stimulated Brillouin scattering (ISBS), and no splitting of dispersion was observed below the lowest-frequency TO mode with $A_1(z)$ symmetry [19]. The experimental results of forward Raman scattering and THz-TDS below $100\,\mathrm{cm}^{-1}$ also did not show any crossing in the dispersion relation [12, 17]. Therefore, it is reasonable to conclude that the resonances of the polariton dispersion observed in the ISRS experiment by Bakker et al. are artifacts.

3.2. Phonon Polariton Dispersion of Lithium Tantalate with A_1(z) Symmetry

In ferroelectric LT crystals, there are four normal modes with $A_1(z)$ symmetry at room temperature. These four modes were clearly observed in both backward Raman scattering and reflection IR spectra [16]. The mode frequencies of four modes are in good agreement with the values reported in literature [14]. By the combination with the observed polariton dispersion relations determined by forward Raman scattering [15, 16], THz-TDS [13] and reflection FTIR spectroscopy, the broadband polariton dispersion relation with $A_1(z)$ symmetry between $10\,\mathrm{cm}^{-1}$ and $1200\,\mathrm{cm}^{-1}$ was determined as shown in Fig. 4. In the reflection FTIR spectra, the complex dielectric constant was determined by the fitting using the damped harmonic oscillator model to determine the dispersion relation of phonon-polariton. The solid lines denote the calculated dispersion with no polariton damping. The values of TO and LO mode frequencies of LT are listed in Table 2. The polariton dispersion of real polariton wavevector is in good agreement with the dispersion observed by forward Raman scattering and THz-TDS, and IR measurements within experimental uncertainty. Regarding the polariton dispersion of the lowest-frequency $A_1(z)$ mode, which is assigned as a ferroelectric soft mode, Penna et al. reported the disappearance of the photon-like linear polariton dispersion below $50\,\mathrm{cm}^{-1}$ for the unpoled lithium tantalate crystal. They discussed this phenomenon by the assumption of the scattering of the polariton propagation by multi-domain structures [20]. On the other hand, in the measurements of forward Raman scattering and THz-TDS, such disappearance of polariton dispersion below $50\,\mathrm{cm}^{-1}$ was not observed in poled crystals [15, 17, 19]. The detailed comparison of observed polariton dispersion among IR, THz-TDS, and Raman measurements of LN and LT crystals will be published separately.

Table 2. Mode frequencies of TO and LO modes with $A_1(z)$ symmetry of a congruent lithium tantalate crystal, where the unit is THz.

	1	2	3	4
ω_{TO}	6.29	7.70	10.8	18.0
ω_{LO}	7.66	10.7	12.1	26.0

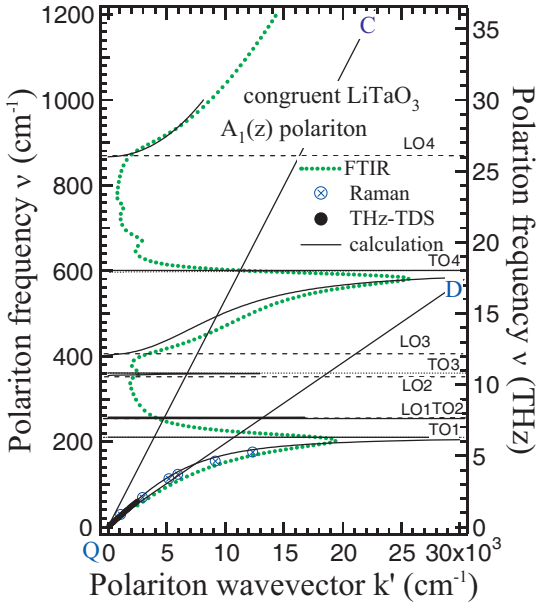

Figure 4. Observed dispersion relation of phonon polariton frequency with $A_1(z)$ symmetry of $LiTaO_3$ against real part of polariton wavevector. The slopes of lines QC and QD are $\frac{1}{\sqrt{\varepsilon_\infty}}$ and $\frac{1}{\sqrt{\varepsilon_0}}$, respectively.

4. CONCLUSION

The broadband dispersion relations of phonon-polariton frequency with infrared and Raman active $A_1(z)$ symmetry of uniaxial lithium niobate and lithium tantalate crystals are important, while till now there is no report on the polariton in the large frequency range between $10\,\mathrm{cm}^{-1}$ and $1200\,\mathrm{cm}^{-1}$. The broadband dispersion relations of phonon-polariton frequency against real part of polariton wavevector were discussed based on the observed results of THz-Raman spectroscopy, THz time domain spectroscopy, and far-infrared spectroscopy.

ACKNOWLEDGMENT

The author is thankful for the collaboration and discussion with Prof. T. Nakamura, Prof. M. Takeda, Prof. M. Maczka, Dr. T. Mori, and Dr. T. Hoshina. This study was supported in part by JSPS KAKENHI Grant Number JP17K05030.

REFERENCES

1. Born, M. and K. Huang, *Dynamical Theory of Crystal Lattices*, Oxford University Press, Oxford, 1954.
2. Claus, R., L. Merten, and J. Brandmüller, *Light Scattering by Phonon-polaritons*, Springer-Verlag, 1975.
3. Xu, Y., *Ferroelectric Materials and Their Applications*, North-Holland, Amsterdam, 1991.
4. Volk, T. and M. Wöhlecke, *Lithium Niobate: Defects, Photorefraction and Ferroelectric Switching*, Springer Series in Materials Science, Vol. 115, Springer, Heidelberg, 2008.
5. Henry, C. H., and J. J. Hopfield, "Raman scattering by polaritons," *Phys. Rev. Lett.*, Vol. 15, 964–966, 1965.
6. Wiederrecht, G. P., T. P. Dougherty, L. Dhar, K. A. Nelson, D. E. Leaird, and A. M. Weiner, "Explanation of anomalous polariton dynamics in $LiTaO_3$," *Ferroelectrics*, Vol. 150, 103–118, 1993.

7. Bond, W. L., "Measurement of the refractive indices of several crystals," *J. Appl. Phys.*, Vol. 36, 1674–1677, 1965.
8. Kojima, S. and T. Nakamura, "Observation of low frequency polaritons in barium sodium niobate," *Jpn. J. Appl. Phys.*, Vol. 19, L609–610, 1980.
9. Kojima, S. and T. Mori, "Terahertz time-domain spectroscopy of infrared active soft mode and phonon-polariton dispersion," *Ferroelectrics*, Vol. 500, 183–202, 2016.
10. Kojima, S., K. Kanehara, T. Hoshina, and T. Tsurumi, "Optical phonons and polariton dispersions of congruent $LiNbO_3$ studied by far-infrared spectroscopic ellipsometry and Raman scattering," *Jpn. J. Appl. Phys.*, Vol. 55, 10TC02-1-5, 2016.
11. Kojima, S., "Composition variation of optical phonon damping in lithium niobate crystals," *Jpn. J. Appl. Phys.*, Vol. 32, 4373–4376, 1993.
12. Kojima, S., H. Kitahara, M. Wada Takeda, and S. Nishizawa, "Terahertz time domain spectroscopy of phonon-polaritons in ferroelectric lithium niobate crystals," *Jpn. J. Appl. Phys.*, Vol. 41, 7033–7037, 2002.
13. Kojima, S., H. Kitahara, S. Nishizawa, and M. Wada Takeda, "Dielectric properties of ferroelectric lithium tantalate crystals studied by terahertz time-domain spectroscopy," *Jpn. J. Appl. Phys.*, Vol. 42, 6238–6241, 2003.
14. Margueron, S., A. Bartasyte, A. M. Glazer, E. Simon, J. Hlinka, I. Gregora, and J. Gleize, "Resolved E-symmetry zone-centre phonons in $LiTaO_3$ and $LiNbO_3$," *J. Appl. Phys.*, Vol. 111, 104105-1–6, 2012.
15. Kojima, S. and T. Nakamura, "Low frequency phonon polaritons in several ferroelectrics," *Ferroelectrics*, Vol. 37, 677–680, 1981.
16. Kojimam, S. and T. Nakamura, "Polariton-spectroscopy in several ferroelectric crystals," *Ferroelectrics*, Vol. 52, 171–180, 1983.
17. Kojima, S., H. Kitahara, S. Nishizawa, and M. Wada Takeda, "Dielectric properties of ferroelectric lithium tantalate crystals studied by terahertz time-domain spectroscopy," *Jpn. J. Appl. Phys.*, Vol. 42, 6238–6241, 2004.
18. Bakker, H. J., S. Hunsche, and H. Kurz, "Coherent phonon polaritons as probes of anharmonic phonons in ferroelectrics," *Rev. Mod. Phys.*, Vol. 70, 523–536, 1998.
19. Crimmins, T. F., N. S. Stoyanov, and K. A. Nelson, "Heterodyned impulsive stimulated Raman scattering of phonon–polaritons in $LiTaO_3$ and $LiNbO_3$," *J. Chem. Phys.*, Vol. 117, 2882–2896, 2002.
20. Penna, A. F., S. P. S. Porto, and E. Wiener-Avnear, "Anomalous polariton dispersion in $LiTaO_3$ near T_C," *Solid State Commun.*, Vol. 23, 377–380, 1977.